

ASSESSMENT OF THE IMPACT OF URBANIZATION GROWTH ON THE CLIMATE OF BAGHDAD PROVINCE USING REMOTE SENSING TECHNIQUES.

¹Sarmad.H. Mahal
Researcher

²A. M. Al-Lami
Assist. Prof.

³F. K. Mashee
Assist. Prof.

¹Department of Astronomy and Space, College of Science, University of Baghdad.

²Atmospheric Sciences of College of Science, Mustansiriyah University.

³Remote Sensing Unit, College of Science, University of Baghdad.

smahal@uomustansiriyah.edu.iq , al.shayia.atmssc@uomustansiriyah.edu.iq

ABSTRACT

This study was aimed to recognize the spatial and temporal features of urban development and its impact on the climate of Baghdad City. The analytical method of the study relies on changes in Land Use/Land Cover (LULC), Normalized Difference Vegetation Index (NDVI), Normalized Difference Built-up Index (NDBI), and Land Surface Temperature (LST); GIS technology was used to measure these statistics. Landsat (5,8) and Sentinel2A imagery were used to detect the change of urbanization growth, vegetation change, and land surface temperature during the study period from 2001 to 2020, whereas used the supervised classification technique for determination for LULC variations. The results showed significant changes among the LULC classes in the studied periods, as most of the LULC changes were caused by human activities. The most prominent changes in LULC were the urban expansion on agricultural land, continuously in all years, which led to the decline of vegetation resulting from land degradation. The Building area increased from around 863 km² in 2001 to 1469 km² in 2020 concentrated mainly in the center, the northeastern and southeastern part of the city. Moderate plants decrease from around 88.5 km² in 2001 to 59 km² in 2020 and dense plants decreased from 0.0252 km² in 2001 to 0.0135 km² in 2020. This has led to negative effects on the climate where temperature rates increased from (26-47) degrees Celsius in 2001 to (32-56) degrees Celsius in the last year of the study, the highest temperatures were recorded in urban growth areas and areas without vegetation.

Keywords: normalized difference built-up index, (LU/LC), land surface temperature (LST), satellite images.

محل وآخرون

مجلة العلوم الزراعية العراقية -2022: 53(5):1021-1034

تقييم أثر النمو العمراني على مناخ محافظة بغداد باستعمال بيانات تقانات التحسس النائي

³ فؤاد كاظم ماشي

² علاء مطر اللامي

¹ سرمد حميد محل

استاذ مساعد

استاذ مساعد

فيزياوي اقدم

¹ قسم الفلك والفضاء - كلية العلوم - جامعة بغداد

² قسم علوم الجو - كلية العلوم - الجامعة المستنصرية

³ قسم التحسس النائي - كلية العلوم - جامعة - بغداد

المستخلص

التحضر هو احد اهم التغيرات البشرية التي احدثها الانسان . تهدف هذه الورقة الى التعرف على السمات المكانية والزمانية للتنمية الحضرية وتأثيرها على مناخ مدينة بغداد . تعتمد الطريقة التحليلية للدراسة على التغير في استخدام الاراضي /الغطاء الارضي LU/LC، ومؤشر الفروق الطبيعي للابنية NDBI، ومؤشر الفروق الطبيعية للغطاء النباتي NDVI، ودرجة حرارة سطح الارض LST، تم استخدام تقنية نظم المعلومات الجغرافية لقياس هذه الاحصائيات ، واستخدمت صور Landsat 8,5 و Sentinel2A للكشف عن عملية النمو الحضري وتغير الغطاء النباتي ودرجة حرارة سطح الارض خلال فترة الدراسة من 2001 الى 2020، واستخدمت تقنية التصنيف الخاضعة للاشراف لتحديد الاختلاف في LULC. اظهرت النتائج تغيرات ملحوظة في فئات LULC خلال فترة الدراسة، معظم تغيرات LULC كانت بسبب الانشطة البشرية . من ابرز التغيرات في LULC هو التوسع الحضري على حساب الاراضي المزروعة بشكل مستمر في جميع السنوات ، مما ادى الى تراجع الغطاء النباتي بسبب تدهور الاراضي. ازدادت مساحة البناء من حوالي 863 كم² في عام 2001 الى 1469 كم² عام 2020 وتركزت بشكل اساسي في وسط المدينة والجزء الشمالي والجنوبي الشرقي من المدينة. انخفضت النباتات المعتدلة من حوالي 88.5 كم² في عام 2001 الى 59 كم² عام 2020 وانخفضت النباتات الكثيفة من 0.025 كم² عام 2001 الى 0.0135 كم² عام 2020، مما ادى الى اثار سلبية على المناخ حيث ارتفعت معدلات درجات الحرارة من (26-47) درجة مئوية عام 2001 الى (32-56) درجة مئوية في عام 2020، سجلت اعلى درجات حرارة في مناطق النمو الحضري والمناطق الخالية من الغطاء النباتي.

الكلمات المفتاحية: معامل الفروق الطبيعية للابنية، استخدام الاراضي/الغطاء الارضي، درجة حرار سطح الارض، صور اقمار صناعية

INTRODUCTION

In most of the major cities in the world, urbanization is a major concern as cities are expanding at an alarming rate because of the migration from rural to urban areas for better job opportunities and living conditions. In 1950, only 30 percent of the global population lived in cities. However, 66 percent of the global population are expected to live in cities in 2050(27). This double rise will lead to many urban problems(12). During the last five decades, urban spatial areas have grown at an accelerated rate, and urban population growth rates are higher than the overall growth in several countries because urban areas are the locus of economic activity and transport nodes(21). The conversion of natural lands into impermeable lands can have a significant impact on the environment. The hydrological system, biodiversity, and local climate may contribute to bad aspects, such as the case of the urban heat island, a status in which the predominant surface temperature in an urban zone is commonly rising than the surface temperature in a neighboring rural zone, with a large temperature variation during nighttime than within midday. The urban spatial growth study and the resulting phenomenon of the urban heat island often require detailed data on urban areas such as scale, shape, and spatial context: therefore, a method is needed to quickly disclose the data. For urban planners and decision-makers, the timely accessibility of data is of great significance. Fortunately, remote sensing satellite technology provides a substantial promise to reach this requirement. Satellites observations can provide global accuracy and repetitive measures of the conditions of the earth's surface with distinct spatial and spectral resolutions(4,31). To distinguish between urban land and non-urban land, several researchers have used remote sensing imagery. The traditional multispectral classification began with a common method for the description of urban areas. However, due to spectral confusion of the heterogeneous Urban land-class built-up, this does not produce satisfactory precision, usually less than 80 percent. Therefore, many studies have not only used a single method of classification to extract the built-up urban lands but have also combined numerous approaches to

improve extraction(21). Remote Sensing is a very active and useful tool that can be used to detect land cover types(6). In recent decades, due to developments in applications for remote sensing and Geographic Information Systems GIS, the usage of has replaced the traditional methods of field surveys for identifying built-up urban land due to advances in remote sensing technology and GIS. In general, satellite imaging techniques for extracting the built-up region can be classified into two groups: Techniques that are based on traditional classification of multispectral images like supervised, object-based, unsupervised, or classification for deep learning (29). Alternate to the classification of images, several researchers have tried normalized indices of difference using particular spectral bands for automatic satellite imagery extraction of built-up ground(31). The built-up land image was produced using the NDBI(32). Significant studies have tried to study land use and shifts in land cover using GIS and remote sensing methods. Anthropogenic behaviors are found to significantly affect the urban climate(3,9,20). Therefore, more efforts are needed to track transitions in LU/LC in urban areas(28). Furthermore, following the replacement of vegetation by urbanized area, climate parameters would also be changed (13,19,30,33). Due to changes in land cover in the US, both the minimum and maximum temperatures rose(17). In Mahmudiyah district, the change in the land cover and land use was found due to human activities in the period 1990-2007, which led to land degradation(7). considered land use and land cover change of the central components for managing natural resources and monitoring environmental changes. In Egypt, the results were urban growth had brought serious losses of agricultural land and water bodies. Urban growth was responsible for a variety of urban environmental issues like decreased air quality, increased runoff, subsequent flooding, increased local temperature, deterioration of water quality, et.(15). The image taken by Landsat 8 of the OLI sensor was used to analyze the NDVI with Arc GIS 10.3. NDVI result showed that it was ranging between (0- - 0.6) in no vegetative cover areas such as water

surfaces and bare soils areas at 2.13% of the total area of Al-Zawra park area in Baghdad city. It was also ranging between (0.4 – 0.3) in areas heavy with large trees planted intensively in that area of 1.25% of the park. Other values ranged between (0.2 – 0.3) of areas planted with less intensive trees them previous of 12.4% of the total area of the park. NDVI ranged (0.1 – 0.2) in areas planted separately with plants where this area formed 60.92% of the total park area. Last category ranged between (0 – 0.1) where it includes light vegetation cover of pale colors including weeds and grasses up to parking lots and empty spaces of (0) NDVI values at 23.30% of the total area of the park (2)The city of Baquba and its outskirts in Diyala province, central Iraq, between latitudes $44^{\circ} 42' 31.78''$ $44^{\circ} 33' 14.99''$ and $33^{\circ} 41' 46.66''$ $33^{\circ} 48' 23.18''$ an area of 180,835 km² has been studied. In order to classify the earth covers, it was relied on the field survey to determine the grounding points, used two satellite data from Landsat 8, the first one on 23/3/2014, the second on 21/3/2019, and the production of (NDVI), (NDWI) and (NDBI) maps. The results of the survey were showed five varieties are vegetation cover, agricultural land, water, buildings and barren land. They were identified and compared with the 75 land control points, The accuracy of the classification was calculated using Kappa It was 89% , and purely concluded that the use of manuals NDVI, NDWI and NDBI was useful for classifying Land coverings and detecting changes as they are considered an easy and fast method (18). According to the literature review above, it is obvious that population growth and subsequent land use and land cover changes have significant adverse effects on the local environment. In general, current

studies have concentrated on exploring bivariate relationships between urbanization and changes in LULC(8,26) , urbanization, and temperature changes (11). Hence, the study aimed to find a relationship between the changes that occurred in the land use/land cover and urbanization, and their effects on climate change, to develop a good strategy to prevent climate fluctuations in the city of Baghdad in the future.

MATERIALS AND METHODS

Description of the study area: Baghdad is located in the central part of Iraq between latitudes 33.452° and 33.184° N, longitudes 44.189° and 44.576° E Figure1, located at an altitude of about 32 meters above sea level, within the flat sedimentary plain sector. Baghdad province includes ten districts and thirty sub-districts, and the borders of the Baghdad Municipality encompass fourteen administrative units, eight in Rusafa (east of the Tigris River) and six in Karkh (west of the Tigris river), with a total coverage area of 870 km². The main characteristics of the study area are large temperature extremism, Low precipitation, low relative humidity, and the sun's high brightness. According to government estimates, the population of Baghdad is more than 8 million (22) and the population is concentrated in the city center. In summer, the region is characterized by a dry and hot climate and a mild climate to cool in spring and winter. The average rainfall is about 150 mm, with the maximum temperature near 40°C in July. Within Baghdad city, there are many industrial projects such as the food industry, paper industry, etc. The city of Baghdad has also busy residential and commercial areas (16).

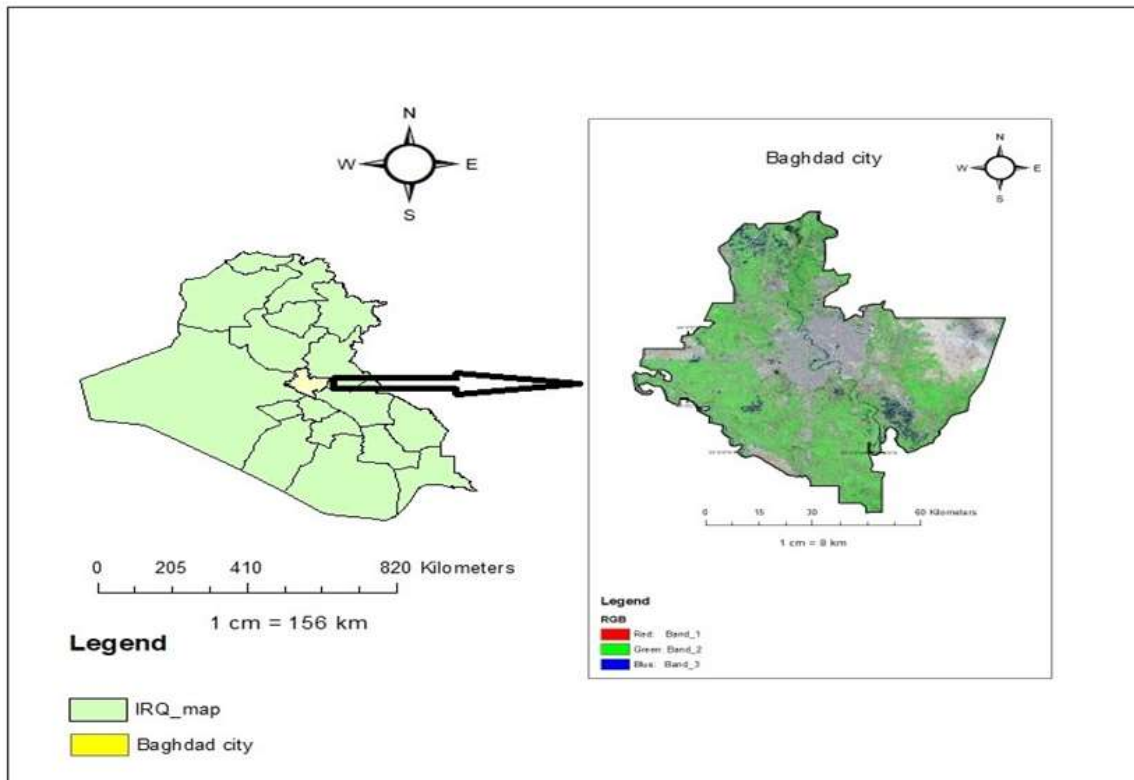


Figure 1. Location of the study area

Data acquisition

Satellite (Landsat 5 with sensor TM (Path/Row: 168 / 037, 169 / 037), Landsat 8 with sensor OLI (Path/Row: 168/ 37, 169/ 37)) data and Sentinel2A with sensor (MSI) have been downloaded from the " USGS website (<https://earthexplorer.usgs.gov>)", to Identifying changes in the vegetation cover, (LU/LC), buildings, and land surface temperature. For two separate years, satellite images were chosen, noting that Sentinel 2 does not have a thermal band, so Landsat 8 images were used to calculating the earth's surface temperature for 2020. The first image is from Landsat 5 in 2001 and the second image in 2020 from Sentinel 2. The data from satellites used in the study is shown in Table 1.

After the images were collected, some digital processing of the satellite images was conducted using GIS 10.7 software to prepare visualizations for the LULC classification, buildings, vegetation, and surface temperature analysis of the land. They were also carried out to transform digital values (DN) into radiance values and reflectance values.

Pre-processing images

Mosaic process were used to merge of two or more Landsat or sentinel images, Baghdad is situated in three areas to scan the Sentinel satellite2 and two areas to scan the Landsat satellite. Study area extraction was applied after completing the mosaic and making as one capture. This method is used to extract the boundaries of the study area Figure 2, 3.

Table 1. The satellite information used for the study

NO	Satellite type	Sensor	Date	Resolution
1	Landsat 5	TM	25-7 & 1-8-2001	30
2	Landsat 8	OLI	13&20-7-2020	30
3	Sentinel 2A	MSI	12&15-7-2020	10-60

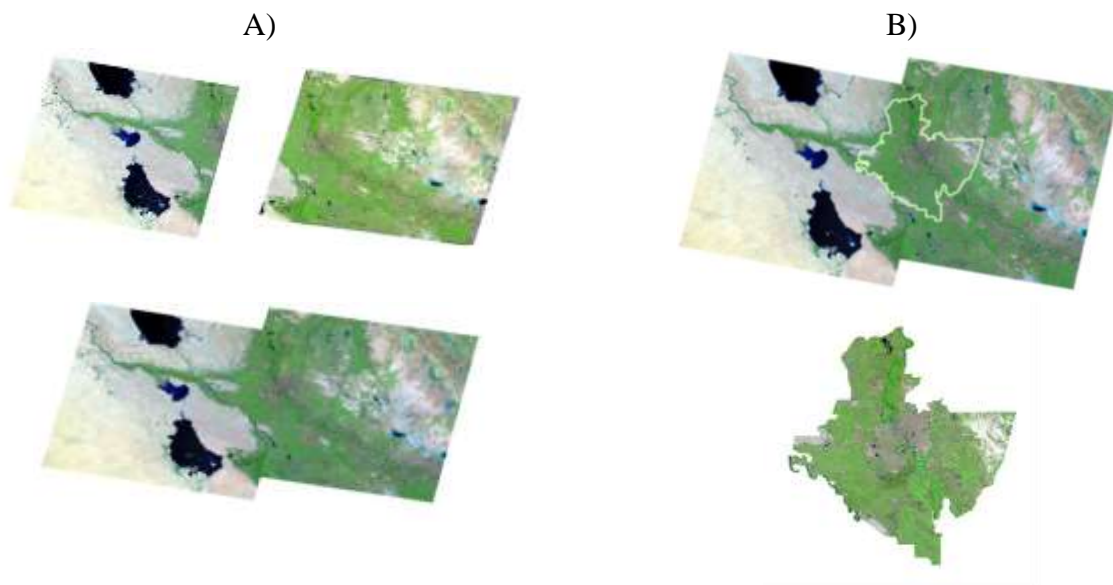


Figure 2. Mosaic images and extraction of Study area images for A,B) Landsat 5

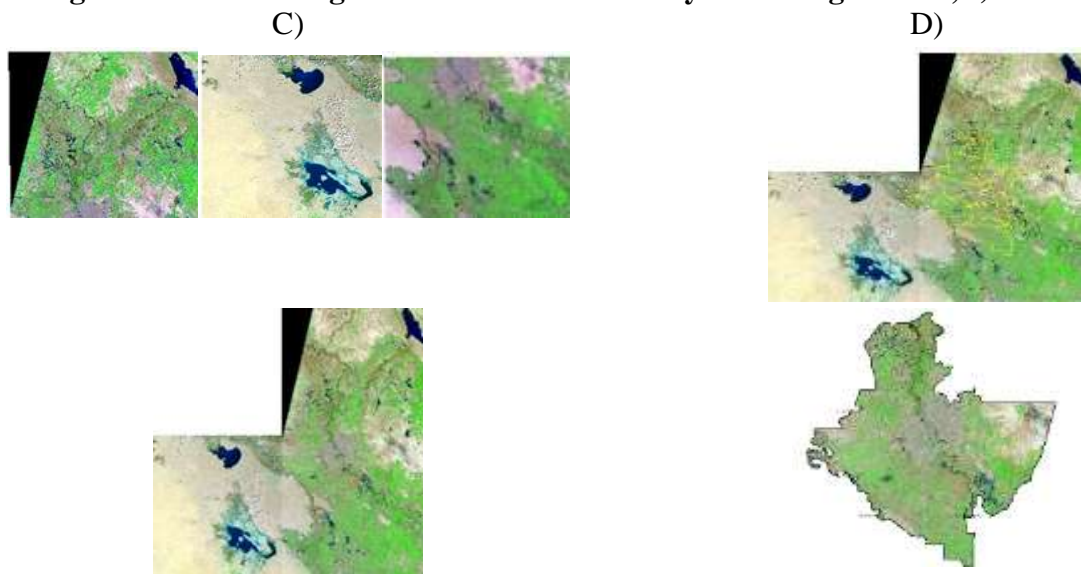


Figure 3. Mosaic images and extraction of Study area images for C,D) sentinel 2

Post-processing images

The changes in Land Use/Land Cover (LULC), Normalized Difference Built-up Index (NDBI), Normalized Difference Vegetation Index (NDVI), and Land Surface Temperature(LST) were used in this study.

Normalized difference built-up index (NDBI)

The built-up land image was generated using the NDBI with the equation below (32).

$$NDBI = \frac{MIR - NIR}{MIR + NIR} \dots \dots \dots (1)$$

$$NDBI \text{ (Landsat 5)} = \frac{B1 - B4}{B1 + B4}$$

$$NDBI \text{ (Landsat 8)} = \frac{B2 - B5}{B2 + B5}$$

$$NDBI \text{ (sentinel 2A)} = \frac{B2 - B8}{B2 + B8}$$

Supervised classification

Land-cover map generation is one of the most common applications in the study of remote sensing images and it is typically accomplished by supervised classification

techniques. These techniques include the availability of accurate ground reference samples to be used in the classification algorithm's learning process. The accuracy of the labeled training samples depends on the quantity and consistency of the availability of the sample (14). There are several methods of supervised classification, and one of these methods has been used in this research called Maximum Likelihood Classification this method is based on Bay's rule if we consider of the phenomena on the surface of the earth with the letter C:

$$C = C_i, C_j, C_k, \dots, C_{nc} \dots \dots \dots (2)$$

Where nc total number of classes, if we take a pixel with vector X to a gray level, the probability of belonging vector x to class Ci given

$$P(C_i | x) \dots \dots \dots (3)$$

If the probability is known to each class, it is possible to determine class Which belongs to pixel with vector X by comparing the possibilities, this can be expressed mathematically by equation:

$$P(C_i | x) > P(C_j | x) \dots\dots\dots (4)$$

The x belongs to class C_i , Since the probability value cannot be directly identified, it can be applied 'Bay rule' provides for P(C_i), is the probability of class C_i and P(x) is the proportion of affiliation pixel to class C_i thus, the equation becomes as follows:

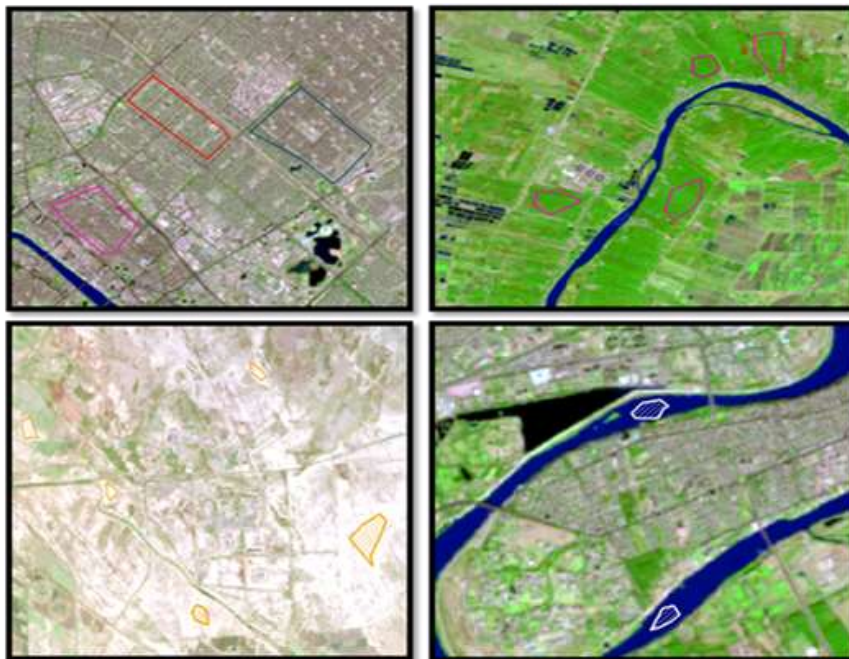
$$P(x) = \sum p(C_i | x) * P(C_i) \dots\dots\dots (5)$$

Where i number of land cover class from 1 to

nc, in this equation we need valuable knowledge P(C_i | x)

$$P(C_i | x) = 1 / [(2\pi)^{1/2} \delta_i] * \exp[- (x - \mu_i)^2 / (2 \delta_i^2)] \dots\dots\dots (6)$$

In this equation we need to find only two coefficients for each class: μ_i which is the mean for the C_i and δ_i which is the standard deviation of C_i class data(24). we choose training samples through field visits and depending on the visual interpretation with Taking into account that the training samples are homogeneous like figures 4 below:



Figures 4 .Training Samples For Study Area

Accuracy Assessment of supervised classification: evaluation of the results of classification is the last and most important step in the classification process as it aims to identify on how well the image units are grouped so that each group has been grouped according to the category represented by reality and quantity to determine the reliability of the results of that classification in different science applications where a number of image units are selected randomly and compared to the results of their classification, if it is the result of the image unit classification corresponds to what it represents on the ground according to the information obtained from the classification, The classification of image unit is correct ,and if we select a number of image units (representing a large proportion of the image) and distributed

appropriately geographically on the image, the result of analyzing the accuracy of this sample of image units can be considered representative of the accuracy of the image classification in general(5). The first step in the process of evaluating the accuracy of the classification is to create " error matrix " and classification accuracy of the space images is calculated using the equation (1).

Accuracy

Assessment=

$$\frac{\text{Total number of matched points in all uses}}{\text{Total random points}} * 100\% \dots\dots (7)$$

The classification accuracy can also be identified using the Kappa coefficient (k), it is a coefficient that measures the extent of the correlation between the actual 27 agreements and the expected agreement by chance. Where if the value of the Kappa coefficient is greater than 0.8, it represents a good accuracy, if it is

between 0.8-0.4, a medium accuracy and if it is less than 0.4, the classification process is poor accuracy This procedure uses all the elements in the error matrix, not just the diagonal(23).

Kappa coefficient

$$\frac{\text{observed accuracy} - \text{chance agreement}}{1 - \text{chance agreement}} \dots\dots(8)$$

Where (observed accuracy) the number of test points matches the real use and the classified map and represents the proportion of total diagonal elements to the number of test points in the error matrix, and (chance agreement) expected by accident and it can be calculated by the equation:

$$\text{Chance agreement} = \sum (\text{Percentage of rated points} * \text{Percentage of points of real use}) \dots(9)$$

Normalized difference vegetation index (NDVI)

To detect the changes related to vegetation, vegetation indices measured from satellite images can be used. The “normalized difference vegetation index (NDVI)” is developed for estimating vegetation cover from the reflective bands of satellite data, and it’s considered as one of the most important geotechnical applications and a means to monitor and interpret changes occurring in the land cover. The NDVI differentiation technique showed the best detection of vegetation change, where plants with high reflectivity in the near-infrared wavelength range and low reflectivity in the red wavelength range are determined by this indicator, The NDVI data layer is defined as(2,25) :

$$NDVI = (NIR - RED) / (NIR + RED) \dots\dots\dots(10)$$

$$NDVI (Landsat 5) = B4 - B3 / B4 + B3$$

$$NDVI (Landsat 8) = B5 - B4 / B5 + B4$$

$$NDVI (sentinel 2A) = B8 - B4 / B8 + B4$$

Calculate the land surface temperature

To extract the (LST) from a satellite image, Band 6 that represented the thermal band for (Landsat 5 with sensor TM) and band 10 for (Landsat 8 with sensor OLI) are used. Converting the digital satellite image values to values for spectral radiation is the first step in measuring the surface temperature of the land. Depending upon the values of spectral radiation (min and max) values from the satellite sensor from the metadata register, the

radiation values are then translated into temperatures (10).

$$L_{\lambda} = \frac{(LMAX_{\lambda} - LMIN_{\lambda})}{QCALMAX - QCALMIN} \times (DN - QCALMIN) + LMIN_{\lambda} \dots\dots(11)$$

Where:

L_{λ} : spectral radiation in [mW cm⁻²sr⁻¹mm⁻¹].

$Lmax_{\lambda} - Lmin_{\lambda}$: spectrum radiation for each range, As its values, are extracted from the Metadata file with the satellite image

DN : Is the pixel DN value

$Qcalmax - Qcalmin$: The value of a digital number of sensor spectral bands from the Metadata.

The DN converted to spectral radiance using the equation:

$$L_{\lambda} = ML * Qcal + AL \dots\dots(12)$$

where:

L_{λ} = Spectral radiance in [mW cm⁻²sr⁻¹mm⁻¹]. ML =Radiance multiplicative scaling factor for the band (RADIANCE_MULT_BAND from the metadata) $Qcal$ = pixel value in DN.

AL =Radiance additive scaling factor for the band (RADIANCE_ADD_BAND_ from the metadata). to convert radiation values to temperatures by using Planck’s Radiance Function.

$$B_{\lambda}(T) = \frac{C_1}{\lambda^5 (e^{\frac{C_2}{\lambda T}} - 1)} \dots\dots\dots(13)$$

Where, $C_1=1.19104356 \times 10^{-16}$ W m², and $C_2=1.43876 \times 10^{-2}$ m K. In the absence of atmospheric effects, T of a ground object can be theoretically determined by inverting the Planck’s function as follows:

$$T = \frac{C_2}{\lambda \cdot \ln \left[\frac{C_1}{\lambda^5 B_{\lambda}(T)} + 1 \right]} \dots\dots\dots(14)$$

reformed this equation get, Let $K1 = C_1/\lambda^5$, and $K2$

C_2/λ , and satellite measured radiant intensity $B_{\lambda}(T) = L_{\lambda}$, then above-mentioned equation is collapsed into an equation:

$$T = \frac{K_2}{\ln \left(\frac{K_1}{L_{\lambda}} + 1 \right)} \dots\dots\dots(15)$$

Where: $K1$ and $K2$ are Values of constants, that vary with the sensor type from the metadata file. (Landsat 5 $K1$ - $K2$: 607.76, 1260.56) and. (Landsat 8 $K1$ - $K2$: 774.8853, 1321.0789). The result of the above equation is the temperature measured in Kelvin unit and

converted them to temperatures measured in Celsius we use the following equation:

$$T(c) = T(k) - 273.15 \dots (16).$$

RESULTS AND DISCUSSION

The ArcGIS Version 10.7 program was used for remote sensing images of Baghdad for the years 2001 and 2020 in July (where July is one of the very hot summer months), the built-up category was more accurately isolated from the rest of the land use/land cover categories from the Landsat 5 and Sentinel 2A images using NDBI equation 1 to detect the status of Spatio-temporal variation over the years in a buildings area in Baghdad city (2001,2020). During the study period, the blue and near-infrared bands were used to display the difference for building blocks. The results are show in Figure 5 and Table 2. The buildings index values showed the spatial and temporal variation in Baghdad during the period 2001 to 2020, where the values ranged from -0.309 to 0.68 in 2001 and from -0.55 to 0.29 in 2020. The unsupervised classification of the built-up maps was introduced. The findings are shown in Table 3 and Figures 6 which show the presence of Spatio-temporal variation in the region of the built-up categories in the study area where the continuous increase in the

built-up category was verified during the study period; the area with buildings in 2001 was 863,1126 km². The area of the built-up category was 1469,4588 square kilometers in 2020, where the growth in the built-up category was 606,3462 square kilometers in the period from 2001 to 2020, Most of this increase was observed in the center of the city on both sides of the Tigris River, such as (Al - Sader 1 District Centre, Al - Sader 2 district Centre, Al – Risafa district Centre, Al - Kadhimiya district Centre, Al - Adhamiya district Centre, Al - Mansour sub-district, etc), in the south such as (Al - Latifya sub-district, etc), in the south-east such as (Al - Mada'in district Centre), the northeast of the city such as (Baghdad Al - Jedeeda sub-district, Al - Fahama sub-district) and also an increase was observed in the north of the city such as the area (Mahmoudiyah). These results corresponded significantly to the reality of the annual rate of population increase in the city of Baghdad, where variation was observed from time to time due to human economic conditions successively affecting Iraq during the study, which had a major effect on urban expansion in the study region as well as on agricultural areas

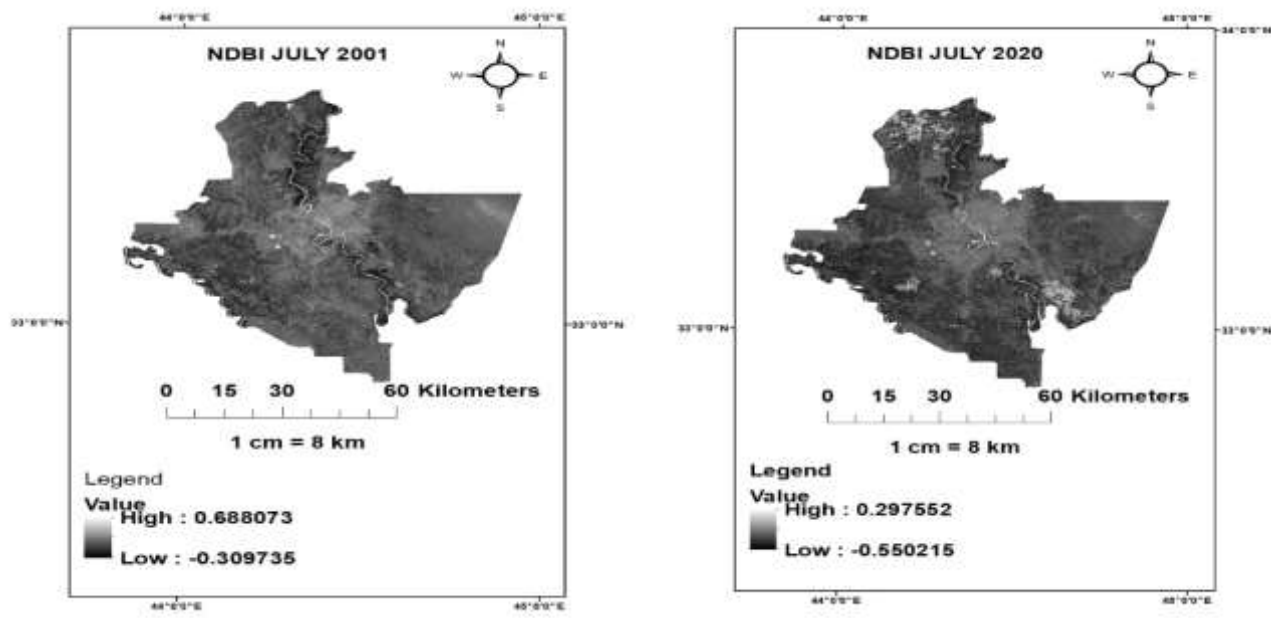


Figure 5. NDBI for Landsat 5 and Sentinel 2A images for (2001,2020)

Table2. NDBI values for the years of study

NO	Year	Min	Max
1	2001	-0.309	0.68
2	2020	-0.55	0.29

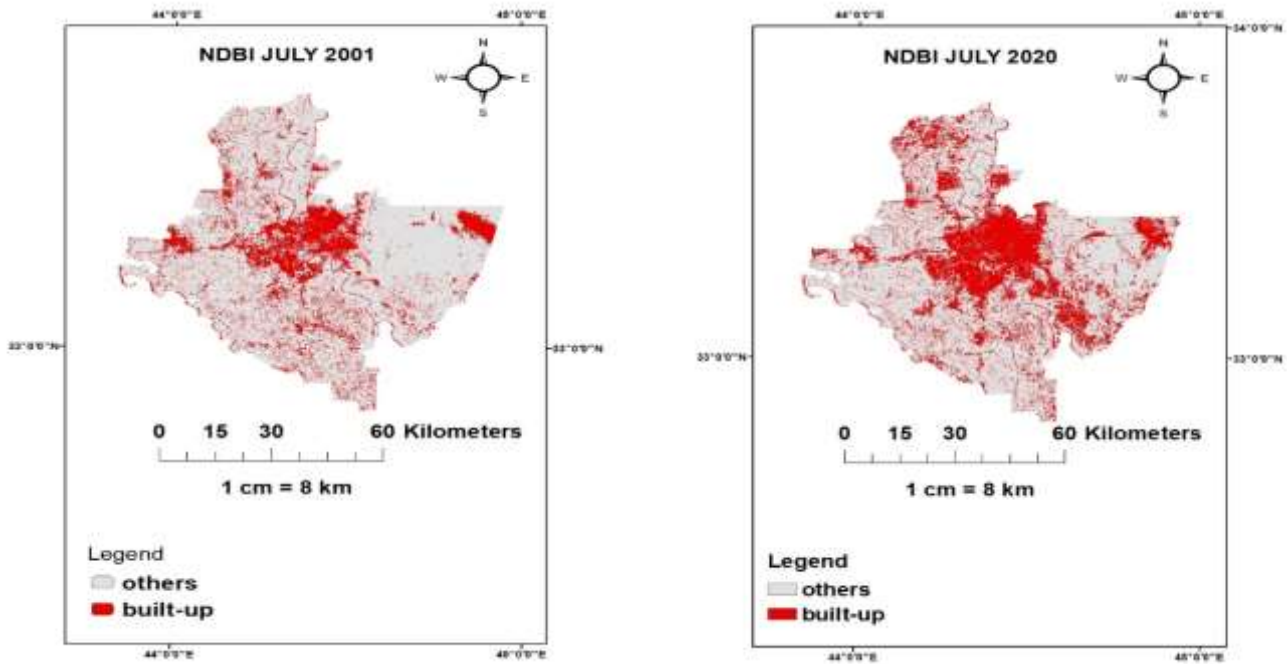


Figure 6. unsupervised classification of the NDBI of Landsat 5 and sentinel 2 images for (2001,2020).

Table 3: The built-up change for the years of study

NO	Year	built-up	others
1	2001	863.1126 km ²	4351.5522 km ²
2	2020	1469.4588 km ²	3745.206 Km ²

Six land use/land cover features (wetlands, scattered plants, land use, dense plants, soil types, water bodies) were established in Baghdad, as shown in Figure 7. To ensure the accuracy of the supervised classification results, the following spectral index values

NDVI, NDWI, BSI, and NDIBI were calculated using ArcGIS version 10.7 for satellite images Landsat5 and sentinel 2A and the years 2001 and 2020. Table 4 shows the land cover/land use for 2001 and 2020.

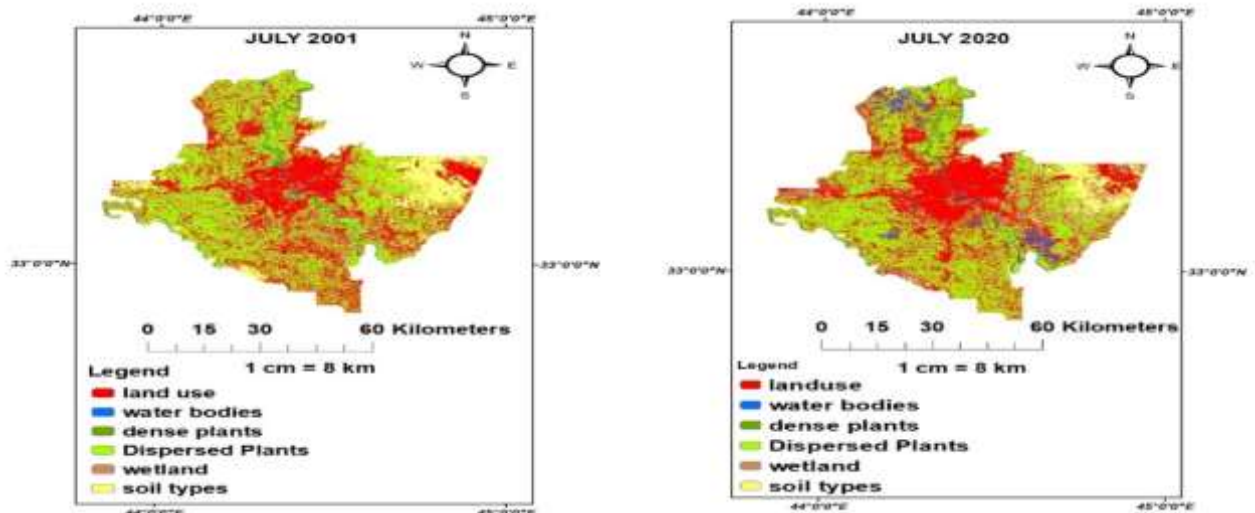


Figure 7. supervised classification on the image (2001,2020)

The results were extracted based on the remote sensing and the Geographic Information Systems methodology to identify changes in LULC in Baghdad city during the years 2001 and 2020. The supervised classification results

showed a variation in LULC due to the climate changes in the region of study in addition to the effects of the human activities showed in Table 4. The results of the supervised classification are shown in Figures 7.

Table 4. The land cover/land use area for periods 2001 and 2020

Class	category	Color	description	Area /km ² 2001	Area /km ² 2020
1	land use		activities of human (commerce, buildings, roads, etc)	1000.6382	2098.3869
2	water bodies		water bodies (natural & industrial)	33.6996	68.1417
3	dense plants		Land cultivated (evergreen)	305.7302	127.6989
4	Dispersed Plants		The natural plants and grass	1652.7573	1054.7419
5	wetland		Lands flooded (temporarily)	1417.8735	170.7537
6	soil types		Barren and salty land	803.8616	1694.9327

Table 5. Error matrixes of Land Use Land Cove from Landsat 5 2001

CLASS	land use	water bodies	dense plants	Dispersed Plants	wetland	soil types	User	accuracy
land use	22	0	0	3	1	0	26	84%
water bodies	0	8	0	0	0	0	8	100%
dense plants	0	0	7	1	0	0	8	87%
Dispersed Plants	0	0	1	32	4	0	37	86%
wetland	0	0	0	1	10	0	11	90%
soil types	1	0	0	0	0	9	8	90%
total	23	8	8	37	15	9		88%

Table 6. Error matrixes of Land Use Land Cove from Sentinel 2A 2020

CLASS	land use	water bodies	dense plants	Dispersed Plants	wetland	soil types	User	accuracy
land use	24	0	0	2	1	2	29	83%
water bodies	0	10	0	0	0	0	10	100%
dense plants	0	0	6	0	1	0	7	86%
Dispersed Plants	0	0	1	29	2	1	33	88%
wetland	0	0	0	1	8	0	9	89%
soil types	1	0	0	0	1	10	12	83%
total	25	10	7	32	13	13		87%

Table 4 shows the first category, land use, increased from 1000.6382 km² in 2001 to 2098.3869 km² in the year 2020. Most of this increase was observed in the following areas of Baghdad: 1) the city center on both sides of the Tigris River, such as Al – Sader1, Al – Sader2, Adhamiya, Kadhimiyah , etc.) the south-east of Baghdad, such as al-Madain and the surroundings, and 3) the northeast of the city such as Al-Fahma. The increase was mainly due to the green and wet areas. The second category represents water bodies which increased from 33.6996 km² in 2001 to 68.1417 km² in 2020 while the third category represents dense vegetation which decreased from 305.7302 km² in 2001 to 127.6989 km² in the year 2020. The fourth category, the dispersed plant, decreased from 1652.7573 km² in 2001 to 1054.7419 km² in 2020. Furthermore, the wetlands, the fifth category,

decreased from 1417.8735 km² in 2001 to 170.7537 km² in 2020. On the other side, the last category which represents soil types increased from 803.8616 km² in 2001 to 1694.9327 km² in 2020, most of this increase was in the east of the city due to the increase of the temperature and aridity.

Accuracy Assessment of supervised classification

Tables (5 and 6) show, respectively, the Error matrixes of Land Use Land Cove, which are resulted from the supervised classification of the Landsat 5 and sentinel 2A satellite image. Validity of this classification results was performed based on the 100 check points, which were used for validation of the classification used in the image. The achieved Overall Accuracy is 88% in 2001 87% in 2020, and a Kappa coefficient is 0.84 in 2001, and 0.833 in 2020. NDVI was used to classify

patterns of vegetation coverage and other types of cover that showed values close to Plant Spectral Reflectivity which impacted the quality of the results Equation no10. Figure 8 displays NDVI values for the 2001 and 2020 images of the study region while Table 7 shows the NDVI at its maximum and minimum. Unsupervised classification, as seen in Figure 9, was applied to the images. For

each image, a vegetation cover area is calculated as seen in Table 4. The NDVI values 0.2-0.4 represent the sparse vegetation, while the NDVI values 0.4-0.6 represent moderate vegetation. Furthermore, the NDVI values in the range 0.6 to 1 range represents dense vegetation. Similarly, the values below 0.2 are the areas of non-vegetation and waterbodies.

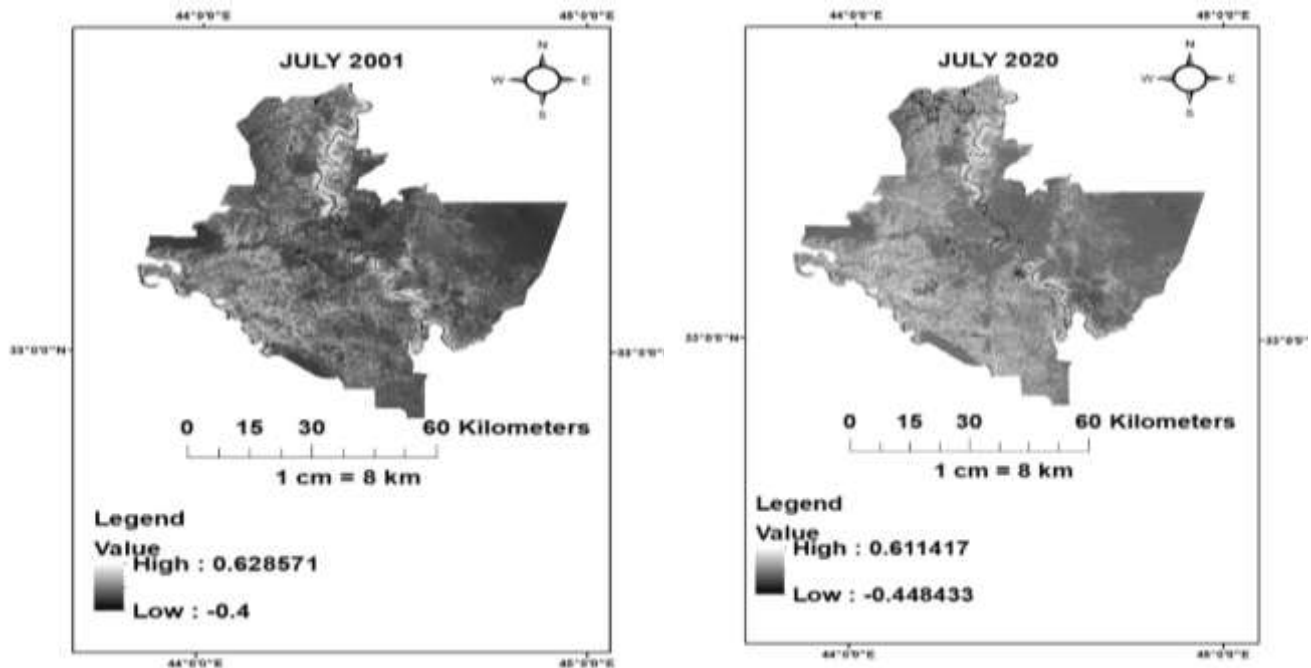


Figure 8. NDVI values for study area 2001 & 2020

Table 7. The Maximum and Minimum values of NDVI for 2001 & 2020 in the study

years /JULY	Maximum	Minimum
2001	0.628	-0.4
2020	0.611417	-0.448433

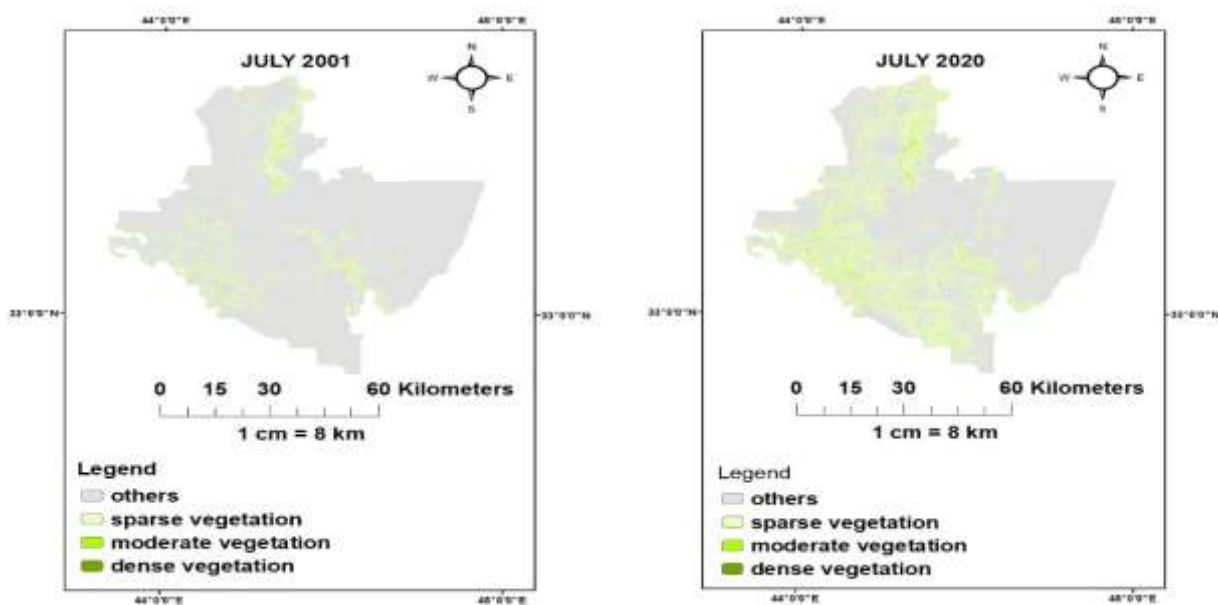
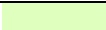


Figure 9. Unsupervised Classification for NDVI (2001,2020).

Table 8. vegetation cover areas in Km²

Class	Color	category	Veg. area (km ²) 2001	Veg. area (km ²) 2020
1		sparse vegetation	793.3743	1216.5102
2		Moderate vegetation	88.4763	59.1354
3		dense vegetation	0.0252	0.0135

From the Landsat (5,8) satellite thermal band, the LST has been determined Figure 10 to calculate the effect of the negative change of the vegetation and to increase buildings on LST. The vegetation degradation process is part of the different degradation cycles faced by natural environments, which affects the natural plant system and reduces its density, and thus affects the overall socioeconomic activity of human beings. Human beings and their activities, including abuse of resources, inadequate planning, and even natural and climatic changes, as low precipitation, elevated temperatures, and drought, are the causes of degradation. Factors such as migrations and the decrease in agriculture work, after that a decrease in cultivated areas, and a decline in economic activities, mainly agriculture, are also causing deterioration. Based on the digital information collected from the analysis of satellite images of vegetation cover in the region of the study and the survey of the field, Table 7 and Figure 8 show that the NDVI values were large in 2001,

as the range is (-0.4-0.628). This indicates a Large vegetation cover in 2001 while its value dropped to (-0.448433-0.611417) in 2020, indicating a significant decrease in the vegetation cover over 19 years. Depending on Table 8 and Figure 9, the area of moderate plants was 88.4763 km² in 2001 and then decreased to 59.1354km² in 2020 while the area of dense plants was 0.0252 km² in 2001 and then decreased to 0.0135km² in 2020. Figure 10 shows that the LST increased from (26-47 degrees Celsius) in 2001 to (32-56 degrees Celsius) in 2020, The highest temperatures were recorded in the east of the city such as (Al - Wihda sub-district Al - Jisr sub-district, etc). the center such as (Al - Karkh district center, Al - Risafa district center, Al - Kadhimiya district center, Al - Adhamiya district center, etc), northeast of the city such as (Al - Zohour sub-district, Al - Fahama sub-district, Baghdad Al - Jedeeda sub-district, etc) and the western part such as the northern part of Al -Nasir & Al-Salam sub-district

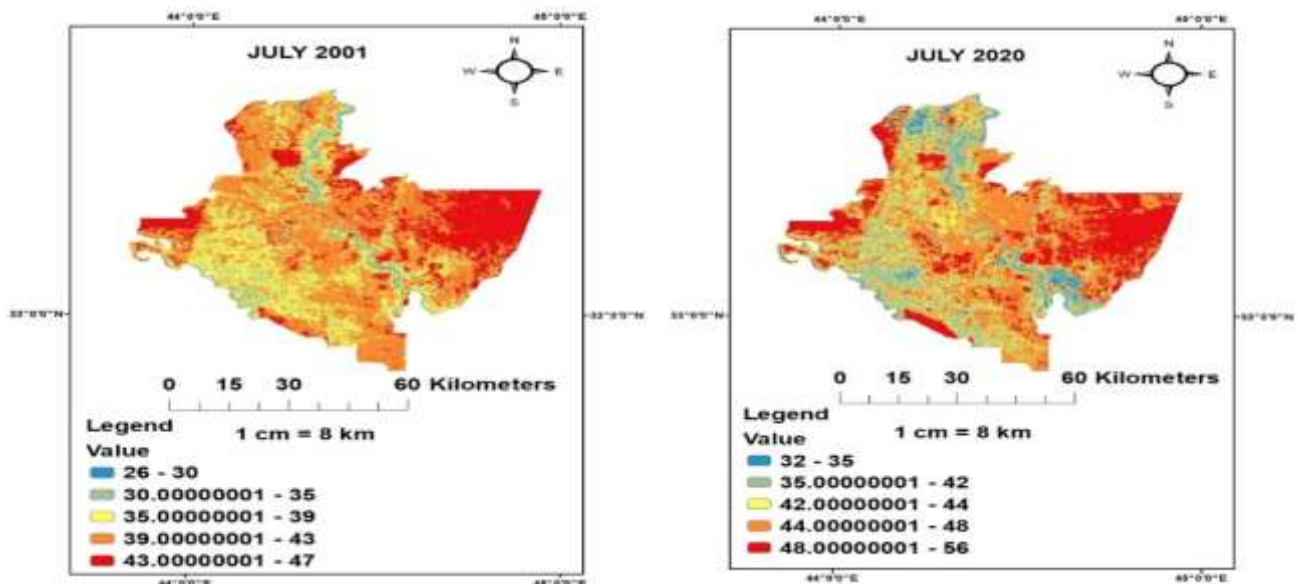


Figure 10. land surface temperature LST (2001,2020)

All these declines in the area of vegetation cover were at the expense of converting agricultural, and open land into populated areas for industrial and commercial uses, in addition to a large number of random settlements that appeared after 2003 in

Baghdad city. The factors that affect the vegetation cover in a study area are desert plants which are the largest part of natural plants, especially in the western and southwest areas of Baghdad, such as herbs and thorns plant.

CONCLUSION

In this study, a statistical method was presented to determine the impact of the change in the land cover/land use and the urbanization on local climate to Baghdad city for July. The results showed the following: the changes in the land cover/land use from 2001 to 2020 affected the local climate due to human activities.

* The study detected a spatial variation of the Buildings and vegetation cover from 2001 to 2020 as follows; the Buildings increased from 863.1126 km² to 1469.4588 km², Moderate vegetation decreased from 88.4763 km² to 59.1354km², dense vegetation from 0.0252 km² to 0.0135 km².

* the increasing temperatures during July, from (26-47 degrees Celsius) in 2001 to (32-56 degrees Celsius) in 2020, Most of the increase was in residential areas and areas devoid of vegetation in the center, east, southeast, and south of the city.

* The NDVI index has an inverse relationship with the surface temperatures of the land, where the area with plant cover (such as the western part of the city) can minimize thermal variation.

* The NDBI index has a positive relationship with the surface temperatures of the land, where the built areas (such as the center of the city), it can increase the temperature. The study found that the use of the spectral indexes method to determine the changes in the land cover/land use was better than the classifications (supervised, unsupervised).

REFERENCES

1. Abdul Rahman Bilal Ali. 2016. Classification of Land Cover around Al-Shari Lake and their Correlation with Climatic Parameters Using Remote Sensing Indicators
2. Al-fatlawi, M. A., and S. N. Jasim. 2019. Study of spatial distribution of vegetation index of alzarwa amusement park in baghdad area using geotechniques. *Iraqi J. Agric. Sci.* 50: 173–181
3. Alberti, M., J. M. Marzluff, E. Shulenberg, G. Bradley, C. Ryan, and C. Zumbrennen. 2003. Integrating humans into ecology: opportunities and challenges for studying urban ecosystems. *Bioscience* 53: 1169–1179
4. Ali, A. K. M., and F. K. M. Al Ramahi. 2020. The Study Air temperature Annual Rates Effect for Urban of Baghdad City by Using Remote Sensing Data Techniques. *Eng. Technol. J.* 38: 66–73
5. Ali, H. Z., and S. N. Al-baldawi. 2015. Performance of Supervised Classification on Landsat images for Mapping Land Cover in Hour AL-Dalmaj Area. 26: 74–77
6. Ali, Z. R., and A. S. Muhaimed. 2016. The study of temporal changes on land cover/land use prevailing in Baghdad governorate using RS and GIS. *Iraqi J. Agric. Sci.* 47: 846–855
7. Aljobory, M. M. and A. 2015. Use of Remote Sensing in the assessment and classification of land degradation in the district of Mahmudiya for the period 1990-2007. *J. Coll. Educ. Women* 26
8. Alqurashi, A. F., and L. Kumar. 2019. An assessment of the impact of urbanization and land use changes in the fast-growing cities of Saudi Arabia. *Geocarto Int.* 34: 78–97
9. Andersson, E. 2006. Urban landscapes and sustainable cities. *Ecol. Soc.* 11
10. Asgarian, A., B. J. Amiri, and Y. Sakieh. 2015. Assessing the effect of green cover spatial patterns on urban land surface temperature using landscape metrics approach. *Urban Ecosyst.* 18: 209–222
11. Chapman, S., J. E. M. Watson, A. Salazar, M. Thatcher, and C. A. McAlpine. 2017. The impact of urbanization and climate change on urban temperatures: a systematic review. *Landsc. Ecol.* 32: 1921–1935
12. Commission, S. P. 2012. Twelfth Five Year Plan. Tamil Nadu 2012-2017. Overview
13. Cui, L., and J. Shi. 2012. Urbanization and its environmental effects in Shanghai, China. *Urban Clim.* 2: 1–15
14. Demir, B., L. Minello, and L. Bruzzone. 2013. Definition of effective training sets for supervised classification of remote sensing images by a novel cost-sensitive active learning method. *IEEE Trans. Geosci. Remote Sens.* 52: 1272–1284
15. Hegazy, I. R., and M. R. Kaloop. 2015. Monitoring urban growth and land use change detection with GIS and remote sensing techniques in Daqahlia governorate Egypt. *Int. J. Sustain. Built Environ.* 4: 117–124
16. Ibrahim, O. A. 2018. Determination of Radon Pollution Regions in Baghdad City

Using Remote Sensing and Geographic Information System. Requir. degree Master Sci. Phys. (RS&GIS), Univ. Baghdad, Coll. Sci. Dep. Phys

17. Kalnay, E., and M. Cai. 2003. Impact of urbanization and land-use change on climate. *Nature* 423: 528–531

18. Khalaf, A. B., and A. I. J. Al-Jibouri. 2020. Detection land cover changes of the baquba city for the period 2014-2019 using spectral indices. *Iraqi J. Agric. Sci.* 51: 805–815

19. Kometa, S. S., and N. R. Akoh. 2012. The Hydro-geomorphological implications of urbanisation in Bamenda, Cameroon. *J. Sustain. Dev.* 5: 64–73

20. Lundholm, J. T., and P. J. Richardson. 2010. MINI-REVIEW: Habitat analogues for reconciliation ecology in urban and industrial environments. *J. Appl. Ecol.* 47: 966–975

21. Masek, J. G., F. E. Lindsay, and S. N. Goward. 2000. Dynamics of urban growth in the Washington DC metropolitan area, 1973-1996, from Landsat observations. *Int. J. Remote Sens.* 21: 3473–3486

22. Mohammed Hashim, B., and M. Abdullah Sultan. 2010. Using remote sensing data and GIS to evaluate air pollution and their relationship with land cover and land use in Baghdad City. *Iran. J. Earth Sci.* 2: 20–24

23. Oldak, A., T. J. Jackson, P. Starks, and R. Elliott. 2003. Mapping near-surface soil moisture on regional scale using ERS-2 SAR data. *Int. J. Remote Sens.* 24: 4579–4598

24. Resler, L. M. 2002. Remote Sensing and Image Analysis

25. Sahebjalal, E., and K. Dashtekian. 2013. Analysis of land use-land covers changes using normalized difference vegetation index

(NDVI) differencing and classification methods. *African J. Agric. Res.* 8: 4614–4622

26. Sajjad, H., and M. Iqbal. 2012. Impact of urbanization on land use/land cover of Dudhganga watershed of Kashmir Valley, India. *Int. J. Urban Sci.* 16: 321–339

27. Spence, M., P. C. Annez, and R. M. Buckley. 2008. Urbanization and growth. World Bank Publications

28. Stow, D. A., and D. M. Chen. 2002. Sensitivity of multitemporal NOAA AVHRR data of an urbanizing region to land-use/land-cover changes and misregistration. *Remote Sens. Environ.* 80: 297–307

29. Vigneshwaran, S., and S. Vasantha Kumar. 2018. Extraction of built-up area using high resolution Sentinel-2A and Google satellite imagery. *Int. Arch. Photogramm. Remote Sens. Spat. Inf. Sci. - ISPRS Arch.* 42: 165–169

30. Voogt, J. A., and T. R. Oke. 2003. Thermal remote sensing of urban climates. *Remote Sens. Environ.* 86: 370–384

31. Xu, H. 2007. Extraction of urban built-up land features from Landsat imagery using a thematicoriented index combination technique. *Photogramm. Eng. Remote Sens.* 73: 1381–1391

32. Zha, Y., J. Gao, and S. Ni. 2003. Use of normalized difference built-up index in automatically mapping urban areas from TM imagery. *Int. J. Remote Sens.* 24: 583–594

33. Zhao, S., L. Da, Z. Tang, H. Fang, K. Song, and J. Fang. 2006. Ecological consequences of rapid urban expansion: Shanghai, China. *Front. Ecol. Environ.* 4: 341–346.